A Noncoherent Model for Microwave Emissions and Backscattering from the Sea Surface

S. T. Wu and A. K. Fung

Space Technology Laboratories, University of Kansas, Lawrence, Kansas 66044

The two-scale (small irregularities superimposed on large undulations) scattering theory proposed by Semyonov has been extended and used to compute the microwave apparent temperature and the backscattering cross section from ocean surfaces. The effect of the small irregularities on the scattering characteristics of the large undulations is included by modifying the Fresnel reflection coefficients, and the effect of the large undulations on those of the small irregularities is accounted for by averaging the scattering cross sections of the small irregularities over the surface normals of the large undulations. The same set of surface parameters in the assumed scattering model is employed at a given wind speed to predict both the scattering and the emission characteristics for both polarizations. Much improved agreement with measured results over a single-surface theory is demonstrated. This agreement indicates that the sea surface is better modeled by a composite than by a single surface. The result also indicates that the adequacy of a scattering model is better exemplified when it is used to predict both the scattering and the emission characteristics.

The microwave emission characteristic of the sea has been measured by several investigators [*Nordberg et al.*, 1969, 1970; *Ross et al.*, 1970; *Hollinger*, 1970, 1971]. These investigators have compared their observations with predictions from the geometric optics theory [*Stogryn*, 1967*b*], which uses a single-surface model, and found some but not satisfactory agreement between predictions and measurements. The wind dependence of the geometric optic approach was based on measured rms sea slope data presented by *Cox and Munk* [1954]. However, the theory failed to predict the observed emission characteristics near nadir and fitted only loosely for nadir angles of 30°–70°. The failure of the geometric optic model to account for wind dependence at nadir was first reported by *Nordberg et al.* [1969] and was verified by *Hollinger* [1971].

In view of the above deficiencies, an investigation is necessary to seek a more adequate model for microwave emissions from the sea. The emphasis in this investigation is oriented toward using a composite-surface model, which better reflects the roughness characteristic of the sea. Since several lengthy numerical integrations are required to yield the emissivity, the more adequate model must not be so complicated that it makes numerical calculations prohibitive. With this perspective, a noncoherent scattering theory of the type described by *Semyonov* [1966] is extended to yield the bistatic scattering coefficient. Since an acceptable scattering coefficient for predicting the microwave emission characteristics must also be acceptable for predicting backscattering, backscattering is examined to provide a cross-check on the model.

To compare with experimental observations, an isotropic surface characteristic, although it is not realistic for the ocean surface, is assumed. A justification for this assumption is based on the observed directional insensitivity of emissions from the sea (Hollinger, private communication, 1971). The two-scale rough surface model is also assumed to have Gaussian surface height distribution and Gaussian surface correlation for both scales. The dielectric constant needed in the calculations is based on the data reported by *Saxton and Lane* [1952].

The wind dependence of the surface parameters in the composite model is introduced in accordance with rms slope data measured by Cox and Munk for the large undulations and *Sutherland*'s [1967] results for the small irregularities. Details for the theory and the choice of surface parameters are given in later sections. Comparisons of the computed brightness temperature and backscattering characteristics at two different wind speeds are made with both measured data and the predictions of a single-surface model.

SURFACE BRIGHTNESS TEMPERATURE THEORY

Formulation of the Problem

The basic theory of apparent surface temperature was developed by *Peake* [1959]. The study that follows concerns only the contribution to the apparent surface temperature due to thermal emission from the sea surface; contributions due to sky radiation reflected from the sea are not considered. The relationship among the surface emissivity, the surface temperature, and the apparent surface temperature (or the surface brightness temperature in this case) is

$$T_{Bj}(\theta) = \epsilon_j(\theta)T_g \qquad j = h, v$$

where $T_{Bj}(\theta)$ is the brightness temperature, $\epsilon_j(\theta)$ is the emissivity, T_g is the surface temperature, h is the horizontal polarization, and v is the vertical polarization. Note that the azimuthal angle ϕ needed together with the nadir angle θ to specify a direction has been chosen to be 0 without loss of generality.

The connection between the emissivity and the differential scattering coefficient of the surface $\gamma_j(\theta, \theta_s, \phi_s)$ is

$$\epsilon_j(\theta) = 1 - \frac{1}{4\pi}\int_0^{2\pi}\int_0^{\pi/2} \gamma_j(\theta, \theta_s, \phi_s) \cdot \sin\theta_s \, d\theta_s \, d\phi_s \qquad (1)$$

where θ_s and ϕ_s are angles defining the direction of scattering corresponding to a wave incident at an angle θ.

The basic formulation of the problem indicated above shows that the differential scattering coefficient is the quantity that defines the angular characteristics of the brightness temperature of a given surface. Consequently, different brightness temperature theories are also distinguished by the different models assumed for the differential scattering coefficient.

Under the noncoherent assumption, $\gamma_j(\theta, \theta_s, \phi_s)$ can be shown [*Semyonov,* 1966] to consist of two terms,

$$\gamma_j(\theta, \theta_s, \phi_s) = \gamma_j^0(\theta, \theta_s, \phi_s) + \langle\gamma_j^1(\theta, \theta_s, \phi_s)\rangle \qquad (2)$$

where $\gamma_j^0(\theta, \theta_s, \phi_s)$ denotes the main contribution by the large undulations and $\langle\gamma_j^1(\theta, \theta_s, \phi_s)\rangle$ denotes the differential scattering coefficient of the small irregularities averaged over the distribution of the surface normals of the large undulations. Detailed derivations for $\gamma_j^0(\theta, \theta_s, \phi_s)$ and $\langle\gamma_j^1(\theta, \theta_s, \phi_s)\rangle$ are given in the following two sections.

Since the backscattering cross section is a special case of the differential scattering coefficients, it can be obtained from the known differential scattering coefficients (Figure 1); i.e.,

$$\sigma_{Bj}^0(\theta) = \cos\theta \cdot \gamma_j(\theta, \theta_s, \phi_s)|_{\substack{\theta_s=\theta \\ \phi_s=\pi}}$$

or equivalently

$$\sigma_{Bj}^0(\theta) = \sigma_{Bj0}^0(\theta) + \langle\sigma_{Bj1}^0(\theta)\rangle \qquad (3a)$$

where

$$\sigma_{Bj0}^0(\theta) = \cos\theta \cdot \gamma_j^0(\theta, \theta_s, \phi_s)|_{\substack{\theta_s=\theta \\ \phi_s=\pi}} \qquad (3b)$$

$$\langle\sigma_{Bj1}^0(\theta)\rangle = \cos\theta \cdot \langle\gamma_j^1(\theta, \theta_s, \phi_s)\rangle|_{\substack{\theta_s=\theta \\ \phi_s=\pi}} \qquad (3c)$$

Detailed derivations of $\sigma_{Bj}^0(\theta)$ are given in the section on backscattering cross sections.

Derivation of $\gamma_j^0(\theta, \theta_s, \phi_s)$

To derive $\gamma_j^0(\theta, \theta_s, \phi_s)$, we begin with the vector-scattered field due to a plane wave incident on an undulating surface to which the tangent plane approximation is assumed applicable. Such a field expression is, in general, rather complicated. To simplify the results, the stationary phase technique will be employed. An expression for $\gamma_j^0(\theta, \theta_s, \phi_s)$ not indicating explicitly the effect of the small irregularities will be derived first. This expression is then clarified to reflect the small structure effects by computing the explicit forms of the modified Fresnel reflection coefficients. As was pointed out by Semyonov, such a computation may be performed for the more general finitely conducting surface in accordance with the work of *Rice* [1951].

Scattered field. The far-zone scattered field in the direction $\mathbf{n}_2$ due to a plane wave polarized along $\mathbf{a}$ impinging on an undulating surface $Z(x, y)$ can be shown to be [*Fung,* 1967]

$$\mathbf{E}_{as} = K\mathbf{n}_2 \times \int \{[(1 + \langle R_h \rangle)(\mathbf{a}\cdot\mathbf{t})(\mathbf{n}\times\mathbf{t}) - (1 - \langle R_v \rangle)(\mathbf{a}\cdot\mathbf{d})(\mathbf{n}\cdot\mathbf{n}_1)t] + \mathbf{n}_2 \times [(1 + \langle R_v \rangle)(\mathbf{a}\cdot\mathbf{d})(\mathbf{n}\times\mathbf{t}) + (1 - \langle R_h \rangle)(\mathbf{a}\cdot\mathbf{t})(\mathbf{n}\cdot\mathbf{n}_1)\mathbf{t}]\} \cdot E_0 \exp[-jk(\mathbf{n}_2 - \mathbf{n}_1)\cdot\mathbf{r}]\, ds \qquad (4)$$

where a time factor of the form $e^{j\omega t}$ has been suppressed and where $K = -jke^{-jkR}/4\pi R$, R is the distance from the origin to the field point, k is the wave number, $\langle R_h \rangle$ and $\langle R_v \rangle$ are the modified Fresnel reflection for horizontal and vertical polarization, respectively, E_0 is the magnitude of incident electric field, $\mathbf{n}_1$ is the unit propagation vector of the incident field, and $\mathbf{n}$ is the normal to the surface.

The set of orthogonal unit vectors ($\mathbf{n}$, $\mathbf{t}$, $\mathbf{d}$) serving as the local coordinates for evaluating the local field on the surface is illustrated in Figure 2. The unit vectors $\mathbf{t}$ and $\mathbf{d}$ relate to $\mathbf{n}$ and $\mathbf{n}_1$ as follows

$$\mathbf{t} = (\mathbf{n}_1 \times \mathbf{n})/|\mathbf{n}_1 \times \mathbf{n}| \qquad \mathbf{d} = \mathbf{n}_1 \times \mathbf{t} \qquad (5)$$

where $\mathbf{n}$ can be written in terms of the partial derivatives Z_x, Z_y of $Z(x, y)$ along the x and y axes as follows

$$\mathbf{n} = (-\mathbf{i}Z_x - \mathbf{j}Z_y + \mathbf{k})/(1 + Z_x^2 + Z_y^2)^{1/2}$$

$\mathbf{i}$, $\mathbf{j}$, $\mathbf{k}$ are the unit coordinate vectors.

To simplify (4) by the stationary phase approximation, let $\mathbf{q} = \mathbf{n}_2 - \mathbf{n}_1$ and q_x, q_y, q_z be the vector components of $\mathbf{q}$. Then the phase factor in (4) is

$$\mathbf{q}\cdot\mathbf{r} = q_x x + q_y y + q_z Z(x, y) \qquad (6)$$

The stationary phase assumption requires that

$$\frac{\partial}{\partial x}(\mathbf{q}\cdot\mathbf{r}) = \frac{\partial}{\partial y}(\mathbf{q}\cdot\mathbf{r}) = 0$$

It follows that

$$Z_x = -q_x/q_z \qquad Z_y = -q_y/q_z \qquad \mathbf{n} = \mathbf{q}/|\mathbf{q}| \qquad (7)$$

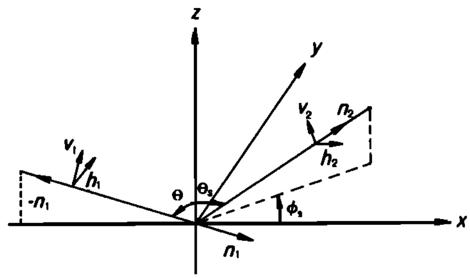

Fig. 1. The sets of orthogonal unit vectors ($-\mathbf{n}_1$, $\mathbf{v}_1$, $\mathbf{h}_1$) and ($\mathbf{n}_2$, $\mathbf{v}_2$, $\mathbf{h}_2$) for expressing the polarization states of the incident and the scattered field.

The significant result indicated by (7) is that all surface slopes in (4) can be written in terms of the incident and scattered propagation vectors. Consequently, the integrand in (4) except for the phase factor exp $[-jk\mathbf{q}\cdot\mathbf{r}]$ can be moved outside the integral sign; i.e.,

$$\mathbf{E}_{as} = E_0 K\mathbf{n}_2 \times \{(\mathbf{A} - \mathbf{B}) + \mathbf{n}_2 \times (\mathbf{C} + \mathbf{D})\} \cdot \int_A \exp[jk(\mathbf{n}_2 - \mathbf{n}_1)\cdot\mathbf{r}]\, ds \qquad (8)$$

where

$$\begin{aligned} \mathbf{A} &= (1 + \langle R_h \rangle)(\mathbf{a}\cdot\mathbf{t})(\mathbf{n}\times\mathbf{t}) \\ \mathbf{B} &= (1 - \langle R_v \rangle)(\mathbf{a}\cdot\mathbf{d})(\mathbf{n}\cdot\mathbf{n}_1)\mathbf{t} \\ \mathbf{C} &= (1 + \langle R_v \rangle)(\mathbf{a}\cdot\mathbf{d})(\mathbf{n}\times\mathbf{t}) \\ \mathbf{D} &= (1 - \langle R_h \rangle)(\mathbf{a}\cdot\mathbf{t})(\mathbf{n}\cdot\mathbf{n}_1)\mathbf{t} \end{aligned} \qquad (9)$$

The local coordinate vectors, two other vector products in (9), and the differential surface element in (8) can all be written in terms of the

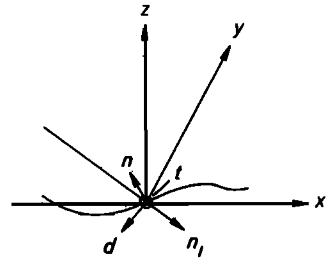

Fig. 2. A set of orthogonal unit vectors ($\mathbf{n}_1$, $\mathbf{t}$, $\mathbf{d}$) serving as the local coordinates for evaluating the local field on surface.

propagation vectors:

$$\mathbf{t} = (\mathbf{n}_1 \times \mathbf{n}_2)/|\mathbf{n}_1 \times \mathbf{n}_2|$$
$$\mathbf{d} = \frac{(\mathbf{n}_1 \cdot \mathbf{n}_2)\mathbf{n}_1 - \mathbf{n}_2}{|\mathbf{n}_1 \times \mathbf{n}_2|}$$
$$\mathbf{n} \times \mathbf{t} = \frac{|\mathbf{n}_2 - \mathbf{n}_1|\,(\mathbf{n}_1 + \mathbf{n}_2)}{2\,|\mathbf{n}_1 \times \mathbf{n}_2|} \tag{10}$$
$$\mathbf{n} \cdot \mathbf{n}_1 = \frac{-|\mathbf{n}_2 - \mathbf{n}_1|}{2}$$
$$ds = (|\mathbf{n}_2 - \mathbf{n}_1|/q_z)\,dx\,dy$$

To express the polarization states of both the incident and the scattered field, it is convenient to introduce a set of orthogonal unit vectors $(-\mathbf{n}_1, \mathbf{v}_1, \mathbf{h}_1)$ for the incident field and another set $(\mathbf{n}_2, \mathbf{v}_2, \mathbf{h}_2)$ for the scattered field (Figure 1). In view of Figure 1, explicit expressions for these unit vectors can be written as

$$-\mathbf{n}_1 = -\sin\theta\mathbf{i} + \cos\theta\mathbf{k}$$
$$\mathbf{v}_1 = \cos\theta\mathbf{i} + \sin\theta\mathbf{k} \tag{11}$$
$$\mathbf{h}_1 = \mathbf{j}$$

$$\mathbf{n}_2 = \sin\theta_s\cos\phi_s\mathbf{i} + \sin\theta_s\sin\phi_s\mathbf{j} + \cos\theta_s\mathbf{k}$$
$$\mathbf{v}_2 = -\cos\theta_s\cos\phi_s\mathbf{i} - \cos\theta_s\sin\phi_s\mathbf{j} + \sin\theta_s\mathbf{k} \tag{12}$$
$$\mathbf{h}_2 = \sin\phi_s\mathbf{i} - \cos\phi_s\mathbf{j}$$

For a horizontally polarized incident wave $(\mathbf{a} = \mathbf{h}_1)$ the polarized and the cross-polarized scattered fields are given, respectively, by

$$\begin{aligned} E_{hh} &= \mathbf{h}_2 \cdot \mathbf{E}_{h_1 s} \\ &= E_0 K[\mathbf{h}_2 \cdot \mathbf{n}_2 \times \{(\mathbf{A}_h - \mathbf{B}_h) + \mathbf{n}_2 \times (\mathbf{C}_h + \mathbf{D}_h)\}] \cdot \int_A \exp[-jk(\mathbf{n}_2 - \mathbf{n}_1)\cdot\mathbf{r}]\,ds \\ E_{hv} &= \mathbf{v}_2 \cdot \mathbf{E}_{h_1 s} \\ &= E_0 K[\mathbf{v}_2 \cdot \mathbf{n}_2 \times \{(\mathbf{A}_h - \mathbf{B}_h) + \mathbf{n}_2 \times (\mathbf{C}_h + \mathbf{D}_h)\}] \cdot \int_A \exp[-jk(\mathbf{n}_2 - \mathbf{n}_1)\cdot\mathbf{r}]\,ds \end{aligned} \tag{13}$$

where

$$\mathbf{A}_h = -|f|\,(1 + \langle R_h\rangle)(\mathbf{v}_1 \cdot \mathbf{n}_2)(\mathbf{n}_1 + \mathbf{n}_2)$$
$$\mathbf{B}_h = |f|\,(1 - \langle R_v\rangle)(\mathbf{h}_1 \cdot \mathbf{n}_2)(\mathbf{n}_1 \times \mathbf{n}_2)$$
$$\mathbf{C}_h = -|f|\,(1 + \langle R_v\rangle)(\mathbf{h}_1 \cdot \mathbf{n}_2)(\mathbf{n}_1 + \mathbf{n}_2)$$
$$\mathbf{D}_h = |f|\,(1 - \langle R_h\rangle)(\mathbf{v}_1 \cdot \mathbf{n}_2)(\mathbf{n}_1 \times \mathbf{n}_2)$$
$$|f| = |\mathbf{n}_2 - \mathbf{n}_1|/2\,|\mathbf{n}_1 \times \mathbf{n}_2|^2$$

Similarly, for a vertically polarized incident wave $(\mathbf{a} = \mathbf{v}_1)$ the polarized and depolarized scattered fields are

$$\begin{aligned} E_{vh} &= \mathbf{h}_2 \cdot \mathbf{E}_{v_1 s} \\ &= E_0 K[\mathbf{h}_2 \cdot \mathbf{n}_2 \times \{(\mathbf{A}_v - \mathbf{B}_v) + \mathbf{n}_2 \times (\mathbf{C}_v + \mathbf{D}_v)\}] \cdot \int_A \exp[jk(\mathbf{n}_2 - \mathbf{n}_1)\cdot\mathbf{r}]\,ds \\ E_{vv} &= \mathbf{v}_2 \cdot \mathbf{E}_{v_1 s} \\ &= E_0 K[\mathbf{v}_2 \cdot \mathbf{n}_2 \times \{(\mathbf{A}_v - \mathbf{B}_v) + \mathbf{n}_2 \times (\mathbf{C}_v + \mathbf{D}_v)\}] \cdot \int_A \exp[jk(\mathbf{n}_2 - \mathbf{n}_1)\cdot\mathbf{r}]\,ds \end{aligned} \tag{14}$$

where

$$\mathbf{A}_v = |f|\,(1 + \langle R_v\rangle)(\mathbf{h}_1 \cdot \mathbf{n}_2)(\mathbf{n}_1 + \mathbf{n}_2)$$
$$\mathbf{B}_v = |f|\,(1 - \langle R_v\rangle)(\mathbf{v}_1 \cdot \mathbf{n}_2)(\mathbf{n}_1 \times \mathbf{n}_2)$$
$$\mathbf{C}_v = -|f|\,(1 + \langle R_v\rangle)(\mathbf{v}_1 \cdot \mathbf{n}_2)(\mathbf{n}_1 + \mathbf{n}_2)$$
$$\mathbf{D}_v = -|f|\,(1 - \langle R_h\rangle)(\mathbf{h}_1 \cdot \mathbf{n}_2)(\mathbf{n}_1 \times \mathbf{n}_2)$$

These field expressions can be simplified further by using the vector identities

$$\mathbf{h}_2 \cdot \mathbf{n}_2 \times (\mathbf{M} + \mathbf{n}_2 \times \mathbf{N}) = \mathbf{v}_2 \cdot \mathbf{M} - \mathbf{h}_2 \cdot \mathbf{N}$$
$$\mathbf{v}_2 \cdot \mathbf{n}_2 \times (\mathbf{M} + \mathbf{n}_2 \times \mathbf{N}) = -\mathbf{h}_2 \cdot \mathbf{M} - \mathbf{v}_2 \cdot \mathbf{N}$$

Thus

$$\begin{aligned} E_{hh} &= C_0(-\langle R_h\rangle bc + \langle R_v\rangle df)I \\ E_{hv} &= C_0(\langle R_h\rangle bf + \langle R_v\rangle dc)I \\ E_{vh} &= C_0(-\langle R_h\rangle df + \langle R_v\rangle bc)I \\ E_{vv} &= C_0(\langle R_h\rangle dc + \langle R_v\rangle bf)I \end{aligned} \tag{15}$$

where

$$C_0 = \frac{-jkE_0 a_1 e^{-jkR}}{2\pi R q_z \, |\mathbf{n}_2 \times \mathbf{n}_1|^2}$$

$$I = \int_A \exp(jk\mathbf{q}\cdot\mathbf{r}) \, dx \, dy$$

$$q_x = \sin\theta_s \cos\phi_s - \sin\theta$$

$$q_y = \sin\theta_s \sin\phi_s$$

$$q_z = \cos\theta + \cos\theta_s$$

$$b = (\mathbf{v}_1 \cdot \mathbf{n}_2) = \sin\theta \cos\theta_s + \cos\theta \sin\theta_s \cos\phi_s$$

$$c = (\mathbf{v}_2 \cdot \mathbf{n}_1) = -\sin\theta \cos\theta_s \cos\phi_s - \cos\theta \sin\theta_s$$

$$d = (\mathbf{h}_1 \cdot \mathbf{n}_2) = \sin\theta_s \sin\phi_s$$

$$f = (\mathbf{h}_2 \cdot \mathbf{n}_1) = \sin\theta \sin\phi_s$$

$$a_1 = |\mathbf{n}_2 - \mathbf{n}_1|^2/2 = 1 + \cos\theta \cos\theta_s - \sin\theta \sin\theta_s \cos\phi_s$$

$$|\mathbf{n}_2 \times \mathbf{n}_1|^2 = (c^2 + f^2) = (b^2 + d^2)$$

Note that by expressing $\mathbf{n}_2$ in terms of the orthogonal set $(\mathbf{n}_1, \mathbf{v}_1, \mathbf{h}_1)$ it can be shown that $|\mathbf{n}_2 \times \mathbf{n}_1|^2 = b^2 + d^2$. Similarly, by expressing $\mathbf{n}_1$ in terms of the orthogonal set $(\mathbf{n}_2, \mathbf{v}_2, \mathbf{h}_2)$ it follows that $|\mathbf{n}_1 \times \mathbf{n}_2|^2 = c^2 + f^2$.

Differential scattering coefficients. The differential scattering coefficients related to the scattered fields computed in the previous section [*Peake*, 1959; *Stogryn*, 1967*a*] are of the form

$$\gamma_{j,i}(\theta, \theta_s, \phi_s) = \frac{4\pi R^2 \langle E_{ji} E_{ji}^* \rangle}{E_0^2 A_0 \cos\theta} \tag{16}$$

where the asterisk denotes the complex conjugate and $\langle \; \rangle$ denotes the ensemble average. The subscripts j and i denote the polarization states of the incident and the scattered fields, respectively. The illuminated area is defined by A_0.

Upon substituting (15) into (16) it follows that

$$\begin{aligned} \gamma_h^0(\theta, \theta_s, \phi_s) &= \gamma_{hh}^0(\theta, \theta_s, \phi_s) + \gamma_{hv}^0(\theta, \theta_s, \phi_s) \\ &= \frac{k^2 a_1^2}{\pi A_0 \cos\theta q_z^2} \cdot \left[\frac{|\langle R_h \rangle|^2 b^2 + |\langle R_v \rangle|^2 d^2}{b^2 + d^2} \right] \langle |I|^2 \rangle \\ \gamma_v^0(\theta, \theta_s, \phi_s) &= \gamma_{vh}^0(\theta, \theta_s, \phi) + \gamma_{vv}^0(\theta, \theta_s, \phi_s) \\ &= \frac{k^2 a_1^2}{\pi A_0 \cos\theta q_z^2} \cdot \left[\frac{|\langle R_v \rangle|^2 b^2 + |\langle R_h \rangle|^2 d^2}{b^2 + d^2} \right] \langle |I|^2 \rangle \end{aligned} \tag{17}$$

For an isotropically rough surface with a Gaussian height distribution, $\langle |I|^2 \rangle$ simplifies to

$$\langle |I|^2 \rangle = 2\pi A_0 \int J_0[k(q_x^2 + q_y^2)^{1/2} \xi] \cdot \exp\{-k^2 q_z^2 \sigma^2 [1 - \rho(\xi)]\} \xi \, d\xi \tag{18}$$

where $J_0(\;)$ is the zero-order Bessel function of the first kind and σ^2 and $\rho(\xi)$ are the variance and the autocorrelation coefficient of the surface, respectively.

An approximate solution for (18) consistent with the stationary phase approximation is

$$\langle |I|^2 \rangle = \frac{2\pi A_0}{k^2 q_z^2 m^2} \exp\left[-\frac{q_x^2 + q_y^2}{2 q_z^2 m^2} \right] \tag{19}$$

where $m = [\sigma^2 |\rho''(0)|]^{1/2}$ is the rms slope of the surface.

Derivation of $\langle \gamma_j^1(\theta, \theta_s, \phi_s) \rangle$

The scattered field due only to the small irregularities has been derived by many investigators [*Rice*, 1951; *Valenzuela*, 1967; *Barrick and Peake*, 1967]. As was indicated in the previous section, when the scattered field expression is known, the scattering coefficient can be computed. To account for the interaction between the small irregularities and the large undulations, the expression for the scattering coefficient of the small irregularities is averaged with respect to the slope distribution of the large undulations. The resulting expression is the desired scattering coefficient $\langle \gamma_j^1(\theta, \theta_s, \phi_s) \rangle$.

Differential scattering coefficients. The far-zone scattered field of i polarization along the direction defined by the angles θ_s' and ϕ_s' due to a plane wave of j polarization with unit amplitude impinging on an irregular surface $s(x, y)$ along the direction defined by the angles θ' and ϕ' has been derived by using the method of small perturbations [*Barrick and Peake,* 1967]. The ensemble average of the magnitude square of the scattered field $\langle |E_{ji}(\theta', \phi', \theta_s', \phi_s')|^2 \rangle$ can be shown to be [*Barrick and Peake,* 1967]

$$\langle |E_{ji}(\theta', \phi', \theta_s', \phi_s')|^2 \rangle = \frac{k^4 A_0}{R^2} \cos^2 \theta' \cos^2 \theta_s' \, |M_{ji}|^2 \, W(p, q) \quad (20)$$

where j and i are incident and scattered polarizations, respectively, either horizontal or vertical polarizations, A_0 is the illuminated area, R is the distance from the field point to the surface, and

$$\begin{aligned} M_{hh} &= \frac{(\epsilon_r - 1) \cos (\phi_s' - \phi')}{[\cos \theta' + (\epsilon_r - \sin^2 \theta')^{1/2}][\cos \theta_s' + (\epsilon_r - \sin^2 \theta_s')^{1/2}]} \\ M_{hv} &= \frac{(\epsilon_r - 1) \sin (\phi_s' - \phi')(\epsilon_r - \sin^2 \theta_s)^{1/2}}{[\cos \theta' + (\epsilon_r - \sin^2 \theta')^{1/2}][\epsilon_r \cos \theta_s' + (\epsilon_r - \sin^2 \theta_s')^{1/2}]} \\ M_{vh} &= \frac{-(\epsilon_r - 1) \sin (\phi_s' - \phi')(\epsilon_r - \sin^2 \theta_s)^{1/2}}{[\epsilon_r \cos \theta' + (\epsilon_r - \sin^2 \theta')^{1/2}][\cos \theta_s' + (\epsilon_r - \sin^2 \theta_s')^{1/2}]} \\ M_{vv} &= \frac{-(\epsilon_r - 1)[\cos (\phi_s' - \phi')(\epsilon_r - \sin^2 \theta')^{1/2}(\epsilon_r - \sin^2 \theta_s')^{1/2} - \epsilon_r \sin \theta_s' \sin \theta']}{[\epsilon_r \cos \theta' + (\epsilon_r - \sin^2 \theta')^{1/2}][\epsilon_r \cos \theta_s' + (\epsilon_r - \sin^2 \theta_s')^{1/2}]} \end{aligned} \quad (21)$$

in which ϵ_r is the complex relative dielectric constant, $W(p, q)$ is the surface roughness spectral density, $p = k [\sin \theta_s' \cos (\phi_s' - \phi') - \sin \theta']$, and $q = k \sin \theta_s' \sin (\phi_s' - \phi')$.

Note that the surface roughness spectral density $W(p, q)$ is related to its correlation function $R(x, y)$ by

$$R(x, y) = \frac{1}{4} \int_{-\infty}^{\infty} \int_{-\infty}^{\infty} W(p, q) \cdot \exp (jpx + jqy) \, dp \, dq$$

For an isotropically rough surface it reduces to

$$R(r) = \frac{\pi}{2} \int_0^{\infty} W(t) J_0(tr) t \, dt$$

and

$$W(t) = \frac{2}{\pi} \int_0^{\infty} R(r) J_0(tr) r \, dr$$

For a Gaussian spectral density it is expressed in the form

$$W(t) = \frac{\sigma_1^2 l^2}{\pi} \exp \left[-\left(\frac{lt}{2} \right)^2 \right] \quad (22)$$

where $t = (p^2 + q^2)^{1/2}$, σ_1 is the standard deviation, and l is the correlation length of the small irregularities.

From (16) and the relation

$$\gamma_j^1(\theta', \phi', \theta_s', \phi_s') = \gamma_{jh}^1(\theta', \phi', \theta_s', \phi_s') + \gamma_{jv}^1(\theta', \phi', \theta_s', \phi_s')$$

we get

$$\gamma_j^1(\theta', \phi', \theta_s', \phi_s') = 4k^4 \sigma_1^2 l^2 \cos \theta' \cos^2 \theta_s' \cdot [|M_{jh}|^2 + |M_{jv}|^2] \exp \left[-\left(\frac{lt}{2} \right)^2 \right] \quad (23)$$

$$j = h, v$$

Averaging procedure. To account for the tilting effect of the small irregularities by the large undulations, it is necessary to average $\gamma_j^1(\theta', \phi', \theta_s', \phi_s')$ with respect to the slope distribution of the large undulations [*Semyonov,* 1966]. That is

$$\langle \gamma_j^1(\theta, \theta_s, \phi_s) \rangle = \int_{-\infty}^{\infty} \int_{-\infty}^{\infty} \gamma_j^1(\theta', \phi', \theta_s', \phi_s') P(Z_x, Z_y) \cdot (1 + Z_x^2 + Z_y^2)^{1/2} \, dZ_x \, dZ_y \quad (24)$$

where θ is the incident angle and θ_s and ϕ_s are the scattering angles.

To evaluate the above integral, connecting relations between the surface slopes Z_x and Z_y and the local angles θ', ϕ', θ_s', and ϕ_s' are needed. To find these relations, let us first express Z_x and Z_y in terms of the azimuth and the elevation angles ϕ_n and θ_n, which represent the tilting effect:

$$\begin{aligned} Z_x &= \cos\phi_n \tan\theta_n \\ Z_y &= \sin\phi_n \tan\theta_n \end{aligned} \tag{25}$$

From (25) it follows that

$$(1 + Z_x^2 + Z_y)^{1/2} = \sec\theta_n$$

$$\begin{aligned} dZ_x\, dZ_y &= \left|\frac{\partial(Z_x, Z_y)}{\partial(\theta_n, \phi_n)}\right| d\theta_n\, d\phi_n \\ &= \sec^3\theta_n \sin\theta_n\, d\theta_n\, d\phi_n \end{aligned} \tag{26}$$

The local angles θ', ϕ', θ_s', and ϕ_s' can now be related to the azimuth and the elevation angles ϕ_n and θ_n by the connecting relations derived below.

In Figure 3, the two sets of coordinates (x, y, z) and (x', y', z') are related in terms of the angles θ_n and ϕ_n as follows:

$$\begin{bmatrix} x' \\ y' \\ z' \end{bmatrix} = \begin{bmatrix} \cos\theta_n \cos\phi_n & \cos\theta_n \sin\phi_n & \sin\theta_n \\ -\sin\phi_n & \cos\phi_n & 0 \\ -\sin\theta_n \cos\phi_n & -\sin\theta_n \sin\phi_n & \cos\theta_n \end{bmatrix} \cdot \begin{bmatrix} x \\ y \\ z \end{bmatrix} \tag{27}$$

Hence, for a scattered field point P located at a distance R from the origin the coordinates of P can be expressed in terms of either the angles θ_s' and ϕ_s' or the angles θ_s and ϕ_s:

$$\begin{aligned} x' &= R \sin\theta_s' \cos\phi_s' \\ y' &= R \sin\theta_s' \sin\phi_s' \\ z' &= R \cos\theta_s' \end{aligned} \tag{28a}$$

or

$$\begin{aligned} x &= R \sin\theta_s \cos\phi_s \\ y &= R \sin\theta_s \sin\phi_s \\ z &= R \cos\theta_s \end{aligned} \tag{28b}$$

Substituting (28) into (27), we obtain the con-

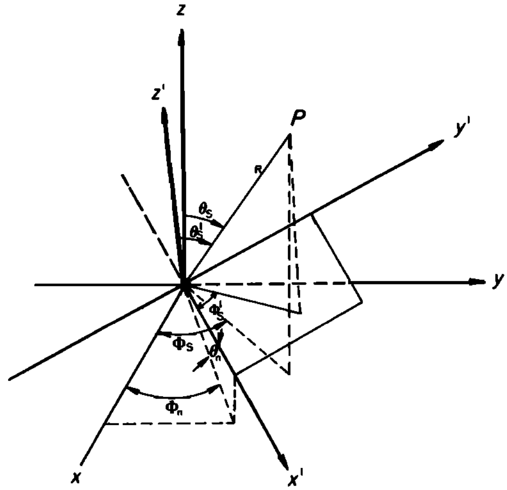

Fig. 3. The azimuthal and the elevation angles ϕ_n and θ_n connecting the two sets of coordinates (x, y, z) and (x', y', z').

necting equations for the sets of angles as follows:

$$\begin{bmatrix} \sin\theta_s' \cos\phi_s' \\ \sin\theta_s' \sin\phi_s' \\ \cos\theta_s' \end{bmatrix} = \begin{bmatrix} \cos\theta_n \cos\phi_n & \cos\theta_n \sin\phi_n & \sin\theta_n \\ -\sin\phi_n & \cos\phi_n & 0 \\ -\sin\theta_n \cos\phi_n & -\sin\theta_n \sin\phi_n & \cos\theta_n \end{bmatrix} \cdot \begin{bmatrix} \sin\theta_s \cos\phi_s \\ \sin\theta_s \sin\phi_s \\ \cos\theta_s \end{bmatrix} \tag{29}$$

If we take the angles with a prime to be local scattering angles, we see from (29) that the local scattering angles can be expressed in terms of the scattering angles θ_s and ϕ_s and the tilting angles θ_n and ϕ_n; i.e.,

$$\begin{aligned} \cos\theta_s' &= \cos\theta_n \cos\theta_s \\ &\quad - \sin\theta_n \sin\theta_s \cos(\phi_s - \phi_n) \\ \sin\phi_s' &= \sin\theta_s \sin(\phi_s - \phi_n) \\ &\quad \cdot (1 - \cos^2\theta_s')^{-1/2} \end{aligned} \tag{30}$$

In a similar fashion the local incident angles can also be expressed in terms of the tilting angles θ_n and ϕ_n and the incident angle θ:

$$\cos\theta' = \cos\theta_n \cos\theta + \sin\theta_n \sin\theta \cos\phi_n$$
$$\sin\phi' = -\sin\theta \sin\phi_n (1 - \cos^2\theta')^{-1/2} \quad (31)$$

When the connecting relations between the local angles and the surface slopes are known, (24) can be evaluated by assuming a form for $P(Zx, Zy)$. For a Gaussian surface slope distribution, $P(Zx, Zy)$ may be represented as

$$P(Zx, Zy) = \frac{1}{2\pi m^2} \exp\left(-\frac{Zx^2 + Zy^2}{2m^2}\right) \quad (32)$$

or equivalently

$$P(\theta_n, \phi_n) = \frac{1}{2\pi m^2} \exp\left(-\frac{\tan^2\theta_n}{2m^2}\right) \quad (33)$$

where m, the rms slope, is assigned according to Cox and Munk's slick sea data.

Since m^2 is usually sufficiently small for the sea and since $\gamma_i^1(\theta', \phi', \theta_s', \phi_s')$ is insensitive to θ_n for small values of θ_n, the integration with respect to θ_n given in (24) can be evaluated by the method of steepest decent, the result being expressed as

$$\langle\gamma_i^1(\theta, \theta_s, \phi_s)\rangle = \frac{1}{2\pi}\int_{-\pi/2}^{\pi/2} \{\gamma_i^1(\theta', \phi', \theta_s', \phi_s')|_{\theta_n = \tan^{-1}(m)} + \gamma_i^1(\theta', \phi', \theta_s', \phi_s')|_{\theta_n = -\tan^{-1}(m)}\}\, d\phi_n \quad (34)$$

Modified Fresnel Reflection Coefficients

As was mentioned earlier, the Fresnel reflection coefficient should be modified to account for the presence of the small irregularities [*Rice*, 1951; *Semyonov*, 1966]. The method for computing these coefficients has been discussed by Rice for horizontally polarized waves. Following Rice's approach, *Valenzuela* [1970] derived the modified reflection coefficient for the vertically polarized waves. However, there appears to be an error in his results, since they differ from Rice's original work by a cosine factor in one of the terms. The corrected modified Fresnel reflection coefficients calculated by Rice's method are

$$\langle R_j\rangle = R_j(\Theta)\left[1 - \tfrac{1}{2}k\cos\Theta \cdot \int_{-\infty}^{\infty}\int_{-\infty}^{\infty} W(u - k\sin\Theta, v) \cdot F_j(u, v)\, du\, dv\right] \quad (35a)$$

$$j = h', v$$

and

$$F_h(u, v) = k(\epsilon_r - \sin^2\Theta)^{1/2} - (c - b) \cdot \left(1 - \frac{v^2}{u^2 + v^2 + bc}\right)$$

$$F_v(u, v) = \frac{\epsilon_r}{\epsilon_r \cos^2\Theta - \sin^2\Theta} \cdot \left[k(\epsilon_r - \sin^2\Theta)^{1/2}\left(1 - \frac{2k\sin\Theta u}{u^2 + v^2 + bc}\right) - \frac{(c - b)}{u^2 + v^2 + bc} \cdot \left(\sin^2\Theta\left\{bc + \frac{u^2}{\epsilon_r}\right\} - u^2\right)\right] - (c - b) \quad (35b)$$

where

$$R_h(\Theta) = \frac{\cos\Theta - (\epsilon_r - \sin^2\Theta)^{1/2}}{\cos\Theta + (\epsilon_r - \sin^2\Theta)^{1/2}}$$
$$R_v(\Theta) = \frac{\epsilon_r \cos\Theta - (\epsilon_r - \sin^2\Theta)^{1/2}}{\epsilon_r \cos\Theta + (\epsilon_r - \sin^2\Theta)^{1/2}} \quad (36)$$
$$\cos\Theta = \frac{1}{(2)^{1/2}}(1 + \cos\theta\cos\theta_s - \sin\theta\sin\theta_s\cos\phi_s)^{1/2}$$

in which ϵ_r is the complex relative dielectric constant and where

$$c = [k^2\epsilon_r - (u^2 + v^2)]^{1/2}$$
$$b = [k^2 - (u^2 + v^2)]^{1/2} \quad (37)$$

For the purpose of this paper the surface roughness spectrum in the above formula is chosen to be

$$W(u - k\sin\Theta, v) = \frac{l^2\sigma_1^2}{\pi} \cdot \exp\left[-\frac{l^2}{4}(u^2 + v^2 - 2ku\sin\Theta + k^2\sin^2\Theta)\right] \quad (38)$$

Backscattering Cross Sections

Substituting $\theta_s = \theta$ and $\phi_s = \pi$ into (36), we obtain

$$R_h(0) = -R_v(0) = \frac{1 - (\epsilon_r)^{1/2}}{1 + (\epsilon_r)^{1/2}} \quad (39)$$

From (17), (19), and (3*b*) it follows that

$$\begin{aligned} \sigma_{Bh_0}{}^0(\theta) &= \frac{|\langle R_h(0)\rangle|^2}{2m^2 \cos^4 \theta} \exp\left(-\frac{\tan^2 \theta}{2m^2}\right) \\ \sigma_{Bv_0}{}^0(\theta) &= \frac{|\langle R_v(0)\rangle|^2}{2m^2 \cos^4 \theta} \exp\left(-\frac{\tan^2 \theta}{2m^2}\right) \end{aligned} \quad (40)$$

To find $\langle \sigma_{Bj1} \rangle$, note the following two points.

1. Substituting $\theta_s = \theta, \phi_s = \pi$ into (30), we obtain

$$\cos \theta_s' = \cos \theta' = \cos \theta_n \cos \theta + \sin \theta_n \cos \phi_n \sin \theta \quad (41)$$

$$\sin \phi_s' = -\sin \phi' = \sin (\phi' + \pi)$$

or

$$\theta_s' = \theta' \qquad \phi_s' = \phi' + \pi$$

2. Since $\theta_s = \theta$ and $\phi_s = \pi$ imply that $\theta_s' = \theta'$ and $\phi_s' = \phi' + \pi$, from (34) it follows that

$$\langle \gamma_j{}^1(\theta, \theta_s, \phi_s)\rangle \Big|_{\substack{\theta_s=\theta \\ \phi_s=\pi}}$$

$$= \frac{1}{2\pi} \int_{-\pi/2}^{\pi/2} \{\gamma_j{}^1(\theta', \phi', \theta_s', \phi_s')\Big|_{\substack{\theta_n=\tan^{-1}(m) \\ \theta_s'=\theta' \\ \phi_s'=\phi'+\pi}} + \gamma_j{}^1(\theta', \phi', \theta_s', \phi_s')\Big|_{\substack{\theta_n=-\tan^{-1}(m) \\ \theta_s'=\theta' \\ \phi_s'=\phi'+\pi}}\} \, d\phi_n \quad (42)$$

Thus from (3*c*) and (42)

$$\langle \sigma_{Bj1}{}^0(\theta)\rangle = \frac{1}{2\pi} \int_{-\pi/2}^{\pi/2} \{\sigma_{Bj1}{}^0(\theta')|_{\theta_n=\tan^{-1}(m)} + \sigma_{Bj1}{}^0(\theta')|_{\theta_n=-\tan^{-1}(m)}\} \, d\phi_n \quad (43)$$

$$j = h, v$$

where

$$\begin{aligned} \sigma_{Bh1}{}^0(\theta') &= \cos \theta' \, \gamma_h{}^1(\theta', \phi', \theta_s', \phi_s')|_{\substack{\phi_s'=\phi'+\pi \\ \theta_s'=\theta'}} \\ &= 4k^4\sigma_1{}^2 l^2 \cos^4 \theta' \, |R_h(\theta')|^2 \\ &\quad \cdot \exp(-k^2 l^2 \sin^2 \theta') \end{aligned} \quad (44)$$

and

$$\begin{aligned} \sigma_{Bv1}{}^0(\theta') &= \cos \theta' \, \gamma_v{}^1(\theta', \phi', \theta_s', \phi_s')|_{\substack{\phi_s'=\phi+\pi \\ \theta_s'=\theta'}} \\ &= 4k^4\sigma_1{}^2 l^2 \cos^4 \theta' \\ &\quad \cdot \left|\frac{(\epsilon_r - 1)[(\epsilon_r - 1)\sin^2 \theta' + \epsilon_r]}{[\epsilon_r \cos \theta' + (\epsilon_r - \sin^2 \theta')^{1/2}]^2}\right|^2 \\ &\quad \cdot \exp(-k^2 l^2 \sin^2 \theta') \end{aligned} \quad (45)$$

The complete backscattering cross section is, of course, given by (3*a*), i.e., the sum of (40) and (43).

SELECTION OF PARAMETERS

The surface parameters that appear in the above theory are the rms slope of the large structures m, the standard deviation of the small structures σ_1, and the correlation length of the small structures l. This scattering model can be adapted to predict sea returns by noting that the rms slope can be based on measurements by *Cox and Munk* [1952] and that the assumed Gaussian spectrum for the small irregularities can approximate the high-frequency part of the sea spectrum BK^{-4}, where the Bragg scatter condition applies, i.e., $K = 2k \sin \theta$. In view of the requirements of the composite-surface theory it is reasonable to choose the oil slick sea measurements by Cox and Munk, since the small irregularities have been suppressed. The value of m is thus assigned. The value of kl is assigned so that the correct angular behavior of the Gaussian spectrum approximated BK^{-4} well over the angular range $30° \leq \theta \leq 70°$; i.e., BK^{-4} is approximated by $\sigma_1^2 l^2/\pi \exp(-K^2 l^2/4)$, where $K = 2k \sin \theta$, the Bragg scatter condition. This approximation is achieved by noting that, when $kl = 2$, similar behavior is realized (Figure 4). The factor 35.3 appears in the Gaussian approximation to bring the levels into agreement at $\theta = 60°$. The value of B must yet be assigned.

Oceanographic investigations indicate values of B in the range from 4.6×10^{-3} to 3.26×10^{-2} [*Cox and Munk*, 1954; *Pierson*, 1970; *Phillips*, 1966]. This implies that $k\sigma_1$ should lie in the range 0.084–0.24 when BK^{-4} is equated to $\sigma_1^2 l^2/4 \cdot \exp(-K^2 l^2/4)$ at $\theta = 60°$. These values of $k\sigma_1$ are consistent with the assumptions of the small-perturbation theory, an encouraging

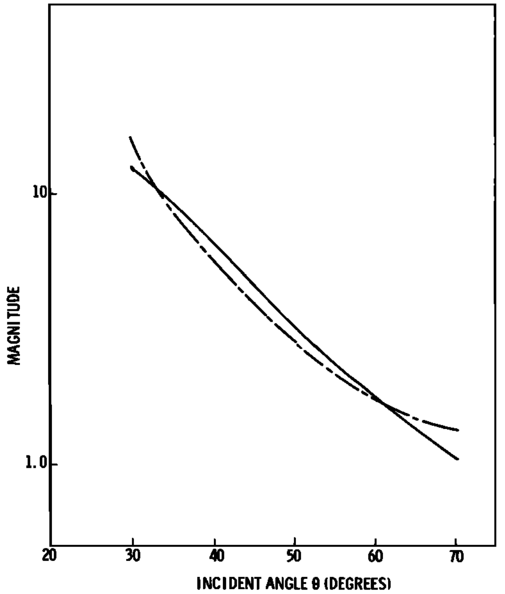

Fig. 4. Comparison of the angular variations of $\sin^{-4}\theta$ (dashed curve) and $35.3 \exp(-4 \sin^2 \theta)$ (solid curve).

result. The recent reports by *Sutherland* [1967] and *Pierson et al.* [1971] indicate that B is a function of the wind speed. Thus the surface parameter $k\sigma_1$ must also be a function of the wind speed. It is noted that the horizontally polarized emission characteristic for nadir angles of 0°–30° is very sensitive to $k\sigma_1$, and hence the parameter $k\sigma_1$ can be estimated by fitting the predicted emission characteristics to the measured data. (It appears that the wind sensitivity of B can be assigned by this technique.)

With the surface parameters established in the manner described above, both the emission and the backscatter characteristics can be computed and compared with reported measurements.

Comparison with Experiments

The parameter $k\sigma_1$ is estimated from horizontally polarized emission characteristics at 8.36 GHz associated with two distinct wind speeds. The emission characteristics are based on an average of several of Hollinger's experiment runs under similar wind stress conditions [*Cardone*, 1969]. The data reported by Hollinger are in the form of surface brightness temperature. Effects due to foam and the reflected sky radiation have been removed [*Hollinger*, 1971]. The vertically polarized emission characteristic is computed from the estimated $k\sigma_1$. These results are shown in Figures 5 and 6. The dielectric constant is based on data reported by *Saxton and Lane* [1952].

Comparison of the predictions of this emission model indicates a significantly improved agreement over that predicted by a single-surface model. Better level and trend agreement is evident for both horizontally and vertically polarized emissions. Sensitivity to wind speed is evident at nadir, which is not noted with the single-surface model. The sensitivity at nadir is carried by the modified Fresnel coefficient (see equation 35).

The adequacy of the composite-surface theory is further demonstrated when the predicted backscatter characteristics are compared with measured characteristics. Data at 8.91 GHz reported by *Daley et al.* [1971] at similar wind stress conditions were chosen as a basis for comparison. The dielectric constant is changed

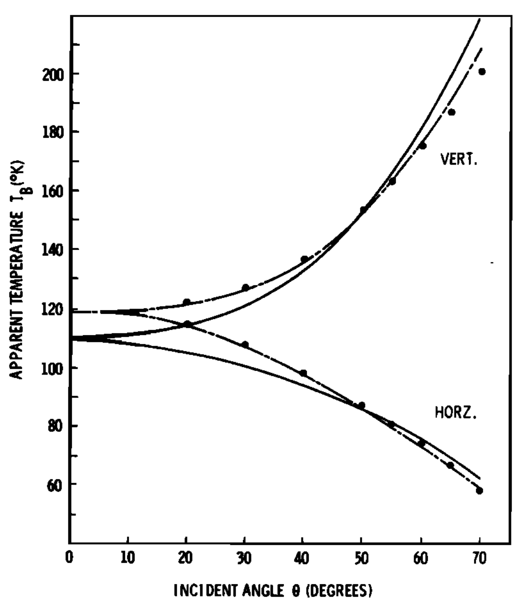

Fig. 5. Comparison of surface brightness temperature for polarized emission characteristics at 8.36 GHz, where $\epsilon_r = 54 - 38.5j$, from Hollinger's data measured at 14.7 knots (solid circles) and the theoretical calculations using single-surface theory for $m = 0.1$ (solid curve) and composite-surface theory for $m = 0.1$, $k\sigma_1 = 0.13$, $kl = 2.0$, $B = 0.9 \times 10^{-2}$ (dashed curve).

to reflect the influence of the slightly different frequency. The comparison of predicted and measured characteristics is shown in Figures 7 and 8. These results indicate reasonable agreement with measurements and improve agreement over the predictions of the simple geometric optic approach (single-surface model). It is noted that the best agreement with measurements occurs primarily at larger angles and for vertical polarization. There is some uncertainty in the accuracy of the measurements near nadir [*Daley et al.*, 1971], and so lack of agreement may be anticipated there. The discrepancy at large angles for horizontally polarized cross sections may be attributable to receiver noise at these small cross sections. This statement is, however, speculative.

The level of the Naval Research Laboratory data based on the statistical median had to be raised by 6 db to realize the agreement. *Valenzuela et al.* [1971] indicated that the average cross section was about 4.6 db above the median based on exponential statistics assumed for the returns. As a consequence, 1.4 db remains unaccounted for. Perhaps the remaining 1.4 db may be partly associated with the biases disclosed by *Claassen and Fung* [1972].

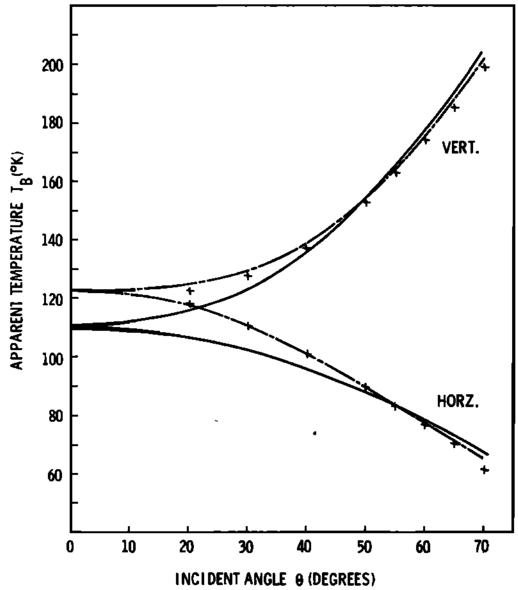

Fig. 6. Comparison of surface brightness temperature for polarized emission characteristics at 8.36 GHz, where $\epsilon_r = 54 - 38.5j$, from Hollinger's data measured at 24.6 knots (crosses) and the theoretical calculations using single-surface theory for $m = 0.12$ (solid curve) and composite-surface theory for $m = 0.12$, $k\sigma_1 = 0.173$, $kl = 2.0$, $B = 1.75 \times 10^{-2}$ (dashed curve).

CONCLUSIONS

A bistatic two-scale noncoherent scattering theory extended from *Semyonov*'s [1966] paper has been developed to yield the expressions for the differential scattering coefficients. The emission and the backscattering characteristics were then derived from the differential scattering coefficients in the standard way. The theory assumed Gaussian surface height distributions and Gaussian correlation functions for both scales of roughness.

The emission and the scattering characteristics are shown to be dependent on the rms slope of the large undulations m, the standard deviation of the small irregularities σ_1, and the correlation length of the small irregularities l. The wind dependence of the first two parameters is associated with m through the slick sea measurements of Cox and Munk, and the σ_1 through the high-frequency sea spectrum. The parameter l is associated with the shape of the high-frequency sea spectrum and can reasonably be chosen by fitting the sea spectrum BK^{-4} to the assumed Gaussian spectrum.

It is noted that the emission characteristic for horizontal polarization is a sensitive measure of σ_1. Thus σ_1 is established by fitting the emission characteristic to the measured data for different wind speeds. The parameters chosen in this way are then used to compute the vertically polarized emission characteristic. Good agreement with measured data and better agreement than is achieved with a simple-surface model are demonstrated.

The same set of surface parameters at each wind speed is then used to compute the backscatter characteristics. The results except for level are shown to agree reasonably with the Naval Research Laboratory backscatter data under similar wind conditions over all angles. Comparison of these characteristics with a single-parameter surface model demonstrated better results.

These findings have proven that the validity of scattering theories is better demonstrated when both the predicted backscatter and the emission characteristics are compared with measurements. They have further shown that

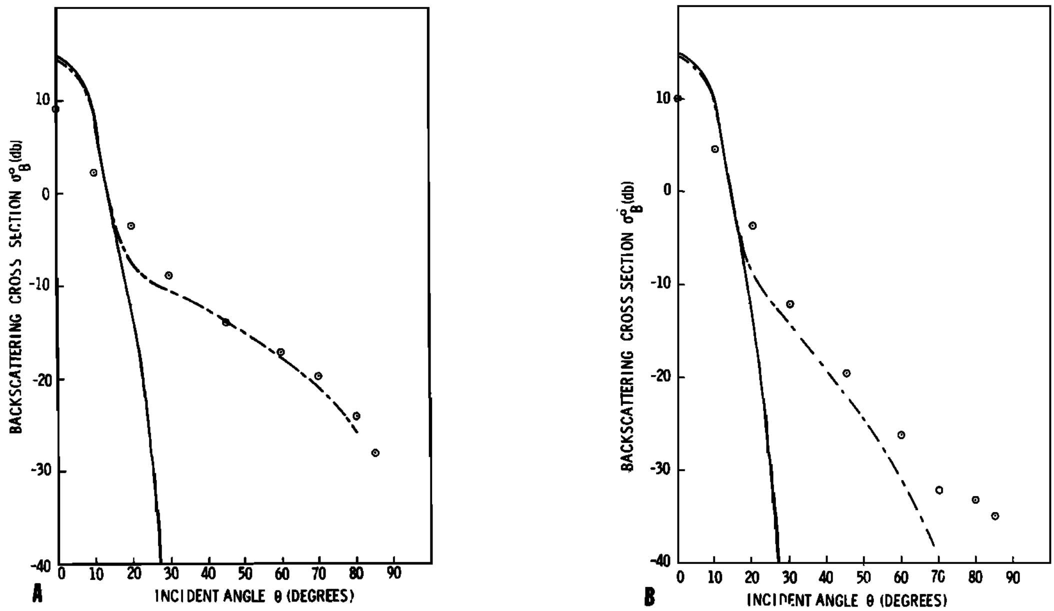

Fig. 7. Comparison of backscattering cross section for (*a*) vertically polarized emission characteristics at 8.91 GHz and (*b*) horizontally polarized emission characteristics at 8.91 GHz from the data of Daley et al. measured at 14–16 knots (circles) and the theoretical calculations using the single-surface theory for $m = 0.10$ (solid curve) and the composite-surface theory for $m = 0.10$, $k\sigma_1 = 0.13$, $kl = 2.0$, $B = 0.975 \times 10^{-2}$, $\epsilon_r = 48.3 - 34.9j$ (dashed curve).

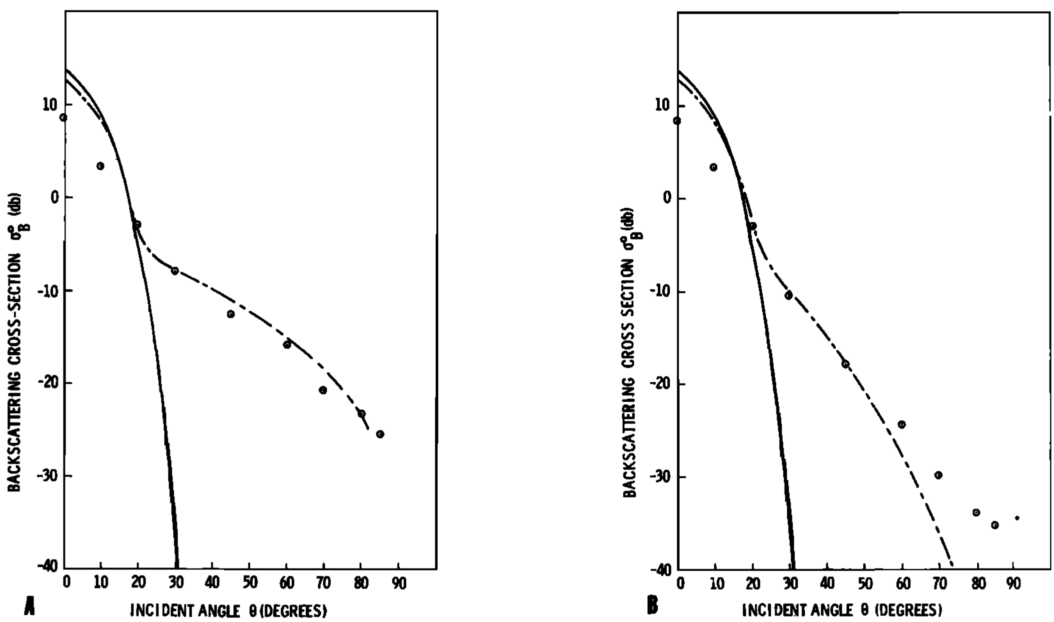

Fig. 8. Comparison of backscattering cross section for (*a*) vertically polarized emission characteristics at 8.91 GHz and (*b*) horizontally polarized emission characteristics at 8.91 GHz from the data of Daley et al. measured at 23–26 knots (circles) and the theoretical calculations using the single-surface theory for $m = 0.12$ (solid curve) and the composite-surface theory for $m = 0.12$, $k\sigma_1 = 0.173$, $kl = 2.0$, $B = 1.75 \times 10^{-2}$, $\epsilon_r = 48.3 - 34.9j$ (dashed curve).

the measured emission and scattering characteristics with the aid of a reasonable composite-surface theory may aid the oceanographer in identifying the wind dependence of the sea spectrum.

Acknowledgment. We are indebted to Dr. J. P. Hollinger of the Naval Research Laboratory for making his radiometric measurements available to us.

This work was supported by the National Aeronautics and Space Administration, Langley Research Center, under contract NAS 1-10048.

REFERENCES

Barrick, D. E., and W. H. Peake, Scattering from surfaces with different roughness scales: Analysis and interpretation, *Res. Rep. BAT-197A-10-3*, Battelle Memorial Inst., Columbus Lab., Nov. 1, 1967.

Cardone, V. J., Specification of the wind distribution in the marine boundary layer for wave forecasting, Ph.D. thesis, N.Y. Univ., University Heights, Dec. 1969. (Also *Tech. Rep. 69-1*, Geophys. Sci. Lab., N.Y. Univ., University Heights, 1969.)

Claassen, J. P., and M. Fung, The wind response of NRL scatterometric observations at *X*-band, *Tech. Rep. 186-5*, Univ. of Kan. Center for Res., Inc., Lawrence, March 1972.

Cox, C., and W. Munk, Statistics of the sea surface derived from sun glitter, *J. Mar. Res., 13*(2), 198–227, 1954.

Daley, J. C., J. T. Ransome, Jr., and J. A. Burkett, Radar sea return–JOSS I, *Rep. 7268*, Nav. Res. Lab., Washington, D.C., May 1971.

Fung, A. K., Theory of cross-polarized power returned from a random surface, *Appl. Sci. Res., 18*, 50–60, 1967.

Hollinger, J. P., Passive microwave measurements of the sea surface, *J. Geophys. Res., 75*(27), 5209–5213, 1970.

Hollinger, J. P., Passive microwave measurements of sea surface roughness, *IEEE Trans. Geosci. Electron., 9*(3), 165–169, 1971.

Nordberg, W., J. Conway, and P. Thaddeus, Microwave observations of sea state from aircraft, *Quart. J. Roy. Meteorol. Soc., 95*, 408–413, 1969.

Nordberg, W., J. Conway, D. B. Ross, and T. Wilhert, Measurement of microwave emission from a foam covered wind driven sea, *NASA Rep. X-650-70-384*, Goddard Space Flight Center, Oct. 1970. (*J. Atmos. Sci., 28*, 429–435, 1971.)

Peake, W. H., Interaction of electromagnetic waves with some natural surfaces, *IEEE Trans., Antennas Propagat., 7*, spec. suppl., S324–S329, 1959.

Phillips, O. M., *The Dynamics of the Upper Ocean*, p. 120, Cambridge University Press, London, 1966.

Pierson, W. J., Jr., A proposed vector wave number spectrum for a study of radar sea return, microwave observations of the sea, *NASA/Navy Rev., SP-152*, 251–282, 1970.

Pierson, W. J., Jr., F. C. Jackson, R. A. Stacy, and E. Mehr, Research on the problem of the radar return from a wind roughened sea, AAFE principal investigator's review, 88–113, Oct. 5–6, 1971.

Rice, D. O., Reflection of electromagnetic waves from slightly rough surfaces, *Commun. Pure Appl. Math., 4*, 361–378, 1951.

Ross, D. B., V. J. Cardone, and J. W. Conaway, Jr., Laser and microwave observations of sea-surface condition for fetch limited 17–25 m/s winds, *IEEE Trans. Geosci. Electron., 8*(4), 326–336, 1970.

Saxton, J. A., and J. A. Lane, Electrical properties of sea water, *Wireless Engr., 29*, 269, 1952.

Semyonov, B., Approximate computation of scattering electromagnetic waves by rough surface contours, *Radio Eng. Electron. Phys., 11*, 1179–1187, 1966.

Stogryn, A., Electromagnetic scattering from rough, finitely conducting surfaces, *Radio Sci., 2*(4), 415–428, 1967*a*.

Stogryn, A., The apparent temperature of the sea at microwave frequencies, *IEEE Trans. Antennas Propagat., 15*(2), 278–286, 1967*b*.

Sutherland, A. J., Spectral measurements and growth rates of wind-generated water waves, *Tech. Rep. 84*, Dep. of Civil Eng., Stanford Univ., Stanford, Calif., Aug. 1967.

Valenzuela, G. R., Depolarization of EM waves by slightly rough surfaces, *IEEE Trans. Antennas Propagat., 15*(4), 552–557, 1967.

Valenzuela, G. R., The effective reflection coefficients in forward scatter from a dielectric slightly rough surface, *IEEE Proc., 58*(8), 1279, 1970.

Valenzuela, G. R., M. B. Laing, and J. C. Daley, Ocean spectra for high frequency waves from airborne radar measurements, *J. Mar. Res., 29*(2), 1971.

(Received November 5, 1971;
revised May 12, 1972.)